# RUNNING HEAD: Flow-mediated dilation and d-sarcoglycan Reduced microvascular flow-mediated dilation in Syrian hamsters lacking d-sarcoglycan is caused by increased oxidative stress

Alexis Richard, Arnaud Bocquet, Eric Belin de Chantemèle, Kevin Retailleau, Bertrand Toutain, Héloïse Mongue-Din, Anne-Laure Guihot, Céline Fassot, Yves Fromes, Daniel Henrion, et al.

SHORT REPORT

RUNNING HEAD: Flow-mediated dilation and δ-sarcoglycan

# Reduced microvascular flow-mediated dilation in Syrian hamsters lacking δ-sarcoglycan is caused by increased oxidative stress

Alexis Richard[1], Arnaud Bocquet[1], Eric Belin de Chantemèle[2], Kevin Retailleau[1], Bertrand Toutain[1], Héloïse Mongue-Din[3], Anne-Laure Guihot[1], Céline Fassot[1], Yves Fromes[3], Daniel Henrion[1], Laurent Loufrani[1].

[1]Univ Angers, Inserm, CNRS, MITOVASC, Equipe CarMe, SFR ICAT, F-49000 Angers, France
[2] Vascular Biology Center, Medical College of Georgia at Augusta University, United States of America; Department of Medicine, Medical College of Georgia at Augusta University, United States of America.
[3]I NMR Laboratory, Neuromuscular Investigation Center, Institute of Myology, Paris, France.

Correspondence: *Laurent Loufrani, Ph.D.*
*MITOVASC, CNRS UMR 6015, INSERM U1083,*
*3 rue Roger Amsler, 49045 Angers, France*
*Tel: +33244688263*
*E-mail: laurent.loufrani@inserm.fr*

## ABSTRACT

δ-sarcoglycan mutation reduces mechanotransduction and induces dilated cardiomyopathy with aging. We hypothesized that in young hamsters with δ-sarcoglycan mutation, which do not show cardiomyopathy, flow mechanotransduction might be affected in resistance arteries as the control of local blood flow.

Flow-mediated-dilation (FMD) was measured in isolated mesenteric resistance arteries, using 3-months old hamsters carrying a mutation in the δ-sarcoglycan gene (CH-147) and their control littermates.

The FMD was significantly reduced in the CHF-147 group. Nevertheless, passive arterial diameter, vascular structure and endothelium-independent dilation to sodium nitroprusside were not modified. Contraction induced by KCl was not modified, whereas contraction due to phenylephrine was increased. The basal NO production and total eNOS expression levels were not altered. Nevertheless, eNOS phosphorylation, FAKs

and RhoA expression were reduced in CH-147. In contrast, p47phox, COX2, iNOS and reactive oxygen species levels were higher in the endothelium of CHF-147 hamsters. Reducing ROS levels using the superoxide dismutase analog Tempol significantly restored the flow-mediated dilation (FMD) levels in CHF-147 hamsters. However, treatment with the COX-2 inhibitor NS-398 showed a non-significant improvement in FMD.

**NEW & NOTEWORTHY**

This study suggests that the sarcoglycan complex is selectively involved in flow-mediated dilation, thus highlighting its role in endothelial responsiveness to shear stress and amplifying tissue damage in myopathy.

**Keywords:** mutation, myopathy, resistance arteries, shear stress

# INTRODUCTION

The dystrophin-glycoprotein complex (DGC) forms a group of transmembranous and membrane-associated proteins mostly located in the sarcolemma of striated muscle cells, as well as in smooth muscle cells. The complex is composed of dystrophin and several sub-classes of proteins (the dystroglycans [$\alpha$ and $\beta$], sarcoglycans [$\alpha, \beta, \gamma$ and $\delta$], sarcospan, the syntrophins [$\alpha 1, \beta 1, \beta 2, \gamma 1, \gamma 2$ (+)], and $\alpha$-dystrobrevin). The complex links the extracellular matrix and cytoskeletal proteins via $\alpha$-dystroglycan, a laminin-associated protein.

Mutations in the sarcoglycan subunit result in muscular dystrophy or sarcoglycanopathy in humans (1, 2). $\delta$-sarcoglycan gene deletion or mutations induce cardiac and skeletal muscle dystrophy characterized by focal necrosis and fibrosis (3). Blood vessels may also be affected by the absence of $\delta$-sarcoglycan (4). Histological analysis of coronary arteries of $\delta$-sarcoglycan -deficient mice shows multiple constrictions along the vascular tree, suggesting the occurrence of vasospasm. In addition, it has been shown that treatment of $\delta$-sarcoglycan deficient mice with a vasodilator restores the smooth appearance of the vascular tree, without focal narrowing of the lumina (5). Although no measurement of blood flow or vascular function was performed in this study, and the vascular defect could possibly be due to smooth muscle and/or endothelial dysfunction.

Smooth muscle cells isolated from Syrian hamsters CHF-147, which lack $\delta$-sarcoglycan, show increased calcium permeability, abnormal proliferation, and apoptosis (6). This, and the above observations, led us to hypothesize that vascular tone might be affected in $\delta$-sarcoglycan -deficient animals. We therefore investigated flow-dependent tone, in resistance arteries isolated from the male CHF-147 Syrian hamsters. Resistance arteries play a key role in peripheral vascular resistance and tissue perfusion (7). Equilibrium in vascular tone allows efficient control of local blood flow in peripheral tissues, and provides a background vascular tone, which increases the effectiveness of circulating and locally produced vasoactive agents.

# MATERIALS AND METHODS

***Animals***

This study was performed on mesenteric resistance arteries (MRAs), from 63 young (three month-old) male δ-sarcoglycan deficient Syrian hamsters (CHF-147, Institut de Myologie, Paris, France) and 63 young (3 month-old) male wild-type Syrian hamsters (RjHan:Aura, Elevage Janvier, France). CHF-147 Syrian hamsters are characterized by a mutation in the δ-sarcoglycan gene that results in the absence of the protein (8, 9). For the FMD study, mice were fed by gavage with SOD-mimetic tempol (4-hydroxy-2,2,6,6-tetramethyl piperidinoxyl) at a dose of 20 mg kg-1 per day for 8 days.

The clinical feature of the δ-sarcoglycan is a " Duchenne like " myopathy (CPK rate very high and EMG confirmed myopathic syndrome). Thus, for this first study, we only used male CHF-147 hamsters because the Duchenne Muscular Dystrophy (DMD) gene responsible for the disease is located on the X chromosome

The animals were sacrificed by $CO_2$ inhalation, and the MRA were gently dissected in physiological solution (PSS) composed of NaCl 130 mM, KCL 78.8 mM, MgSO4 (7H20) 1.2 mM, NaHCO3 14.9 mM, HEPES 5 mM, kH2PO4 1.2 mM, D-glucose 11 mM D-glucose) at 4°C with a physiological pH of 7.4 ($\pm$ 0.2).

**Ethics Statement:**

The procedure followed in the care and euthanasia of the study animals was in accordance with the European Community Standards on the Care and Use of Laboratory Animals (Ministère de l'Agriculture, France, authorization No. 6422) and with the principles of laboratory animal care (NIH publication no. 85–23, revised 1985). The protocol was approved by the ethical committee (Protocol CEEA PdL #2008.10).

***Pressure myography - Flow-dependent tone in mesenteric arteries***

Segments of MRAs were cannulated at both ends and mounted in a video-monitored perfusion system, as previously described (10). Briefly, cannulated arterial segments were bathed in a 5 ml organ bath containing the PSS solution with a pH of 7.4, a pO2 maintained at 160 mmHg, and a pCO2 maintained at 37 mmHg (10). The arterial diameter was recorded continuously using the video monitoring system (Living System Instrumentation Inc., Burlington, VT). Intraluminal pressure and flow rate could be changed independently. Arteries were submitted to a pressure of 75 mmHg and further contracted with phenylephrine (PE, 50% of initial diameter) to maintain a stable and reproducible tone in the different groups. Intraluminal flow was then increased step by step (3 µl/min to 100 µl/min) and the diameter measured. At the end of each experiment, arteries were perfused and superfused with a $Ca^{2+}$-free PSS containing ethylenebis-(oxyethylenenitrolo) tetra-acetic acid (EGTA, 2 mmol/L), sodium nitroprusside (10 µmol/L) and papaverin (10 µmol/L). Pressure (ranging from 10 to 150 mmHg) was then increased step by step to determine the passive diameter of the vessel, i.e., in the absence of smooth muscle tone. Pressure and diameter measurements were collected using a Biopac data acquisition system (Biopac MP 100, La Jolla, CA, USA) and analyzed (Acqknowledge® software, Biopac). FMD was calculated as percentage of passive diameter (10). NS-398 was used at $10^{-5}$ M in MRA flow-mediated dilation. Before each experiment, the contractility of the muscle was tested using PE (10 µmol/L), and the integrity of the endothelium was assessed by testing the relaxing effect of acetylcholine (ACh, 1 µmol/L) (10).

***Wire myography - Pharmacological properties of resistance arteries***

Segments of MRAs (2 mm long) were dissected in PSS and mounted on a wire-myograph (DMT, Aarhus, DK) as previously described (10). Briefly, 2 tungsten wires (25 µm diameter) were inserted into the artery lumina; one wire was fixed to a force transducer, the other to a micrometer. Arteries were bathed in a PSS as described above and maintained at 37°C, pH 7.4, $pO_2$ 160 mm Hg, $pCO_2$ 37 mm Hg. Wall tension was applied as previously described (11). Vessels were then allowed to stabilize for one hour. Artery viability was tested using a potassium-rich solution (80mol/L, 80K PSS). The endothelium was considered functional when an 80% ACh-induced relaxation ($10^{-6}$M) was obtained after PE-induced preconstriction (50% of maximal contraction with KCL 80 mM). A cumulative concentration-response curve (CRC) to PE ($10^{-9}$-$10^{-4}$ M) was constructed. Finally, a CRC to sodium nitroprusside (SNP, $10^{-9}$-$10^{-5}$M) after PE-induced preconstriction ($10^{-6}$ M) was constructed.

***Western blot analysis***

Western blot analysis was performed on MRAs as previously described (12). Briefly, pooled MRAs (3 per animal) were homogenized using a lysis buffer (1% sodium dodecyl sulfate [SDS], 10 mmol/L Tris-HCl [pH 7.4], 1 mmol/L sodium orthovanadate, 2.5 mg/L leupeptin and 5 mg/L aprotinin). Extracts were incubated at 4°C for 30 minutes and then centrifuged (14 000 rpm, 15 minutes, 14°C). The protein concentration was determined using the Micro BCA Protein Assay Kit (Pierce). After denaturation at 95°C for 5 minutes, equal amounts of protein (25 µg) were loaded onto a 9% polyacrylamide gel and transferred to nitrocellulose membranes for 90 minutes (100 V, 4°C). Membranes were blocked with 5% bovine albumin (BSA) in Tris-buffered saline Tween 20 (TBST) (20 mmol/L Tris [pH 8.0], 150 mmol/L NaCl, and 0.1% Tween-20) for 1 hour; they were then incubated with the primary antibody in 5% BSA in TBST overnight at 4°C. After extensive washing in T-TBS at room temperature, membranes were then incubated with secondary antibody for 90 minutes at room temperature. After 3 washes with TBST, immunocomplexes were detected by chemiluminescent reaction (ECL-kit; Amersham Pharmacia Biotech) using a computer-based imaging system (Fuji LAS 3000 plus; Fuji Medical System). Quantification was performed by densitometric analysis and normalized by β-actin signal.

Antibodies were used as follows: eNOS 1/1000 (9572 Cell signaling); phospho-eNOS Ser1177 1/1000 (9571 Cell signaling); Akt 1/1000 (9272 Cell signaling); phospho-Akt Ser473 1/1000 (4060 Cell signaling); PI3Kp85 1/500 (4292 Cell signaling); P47 1/500 (PA1-9073 Thermofisher); focal adhesion kinase (FAK) 1/500 (ab40794 Abcam); β-actine 1/1000 (A5316 Sigma-Aldrich); anti-rabbit 1/4000 (NA934 Amersham Pharmacia Biotech, Orsay, France) or anti-mouse 1/4000 horseradish peroxidase antibody (NA931 Amersham Pharmacia Biotech, Orsay, France).

***Histomorphometric analysis***

Segments of MRAs were fixed in 4% paraformaldehyde at 75 mmHg and were mounted in embedding medium (Tissu-Tek, Miles, Inc), frozen in isopentane pre-cooled in liquid nitrogen, and stored at -80°C. Transverse sections (7 µm thick) of MRA were stained with orcein solution. Media thickness, and internal and external medial circumferences were measured. The media-to-lumen ratio was calculated as previously described (10).

### *Immunofluorescence analysis*

Segments of 7 μm thick cross sections of MRAs were mounted in embedding medium (Miles, Inc), frozen in isopentane pre-cooled in liquid nitrogen, and stored at -80°C. Sections were incubated with cyclooxygenase (COX)-2 or iNOS (1/200 each, overnight, 4°C), rinsed for five minutes three times, and then incubated with the secondary antibody (Alexa 488 nm, 1/200) for 90 minutes. Fluorescent staining was visualized using confocal microscopy (Solamere Technology, Salt Lake City, UT, USA). Image analysis was performed using Histolab (Microvision, France). Briefly, pixel quantification was performed after separating the endothelial layer.

### *Reactive oxygen species (ROS) detection*

Superoxide anion detection was performed on 7 μm thick artery cross sections incubated with dihydroethidine (DHE) as previously described (13, 14). Positive staining was visualized using confocal microscopy and QED-image software (Solamere Technology, Salt Lake City, UT). Image analysis was performed using Histolab (Microvision, France). Pixel quantification was carried out as previously described (14). A positive control was performed using sections of MRA treated with lipopolysaccharide in vitro in the PSS at 37°C for 2 hours. A negative control was obtained by omitting DHE or by adding tempol to the sections 15 min before DHE.

### *Statistical analysis*

Results are expressed as mean ± SEM. Significance of the differences between groups was determined by analysis of variance (2-way ANOVA for consecutive measurements, when appropriate) or Mann Whitney test for two groups analysis. P values less than 0.05 were considered as significant.

## RESULTS

### *Flow-mediated dilation is decreased in mesenteric arteries from CHF-147 hamsters*

When pressure was maintained at 75 mmHg and after 50% of basal diameter contraction with PE, increasing flow step-by-step resulted in dilation in control arteries (Figure 1). In CHF-147 hamsters, flow (shear stress)-induced dilation was significantly attenuated in mesenteric resistance arteries (Figure 1).

### *The δ-sarcoglycan deficiency does not impact vascular structure and reactivity of mesenteric arteries*

No significant change was found in passive arterial diameter (Figure 2A), lumen area, media area internal diameter or media to lumen ratio area in mesenteric resistance arteries, reflecting no vascular remodeling (Figure 2B). Moreover, no significant change was observed between the two groups in endothelium-dependent dilation (Figure 2C), endothelium-independent dilation (Figure 2D and E), concentration-dependent inhibition of NO synthesis by L-NAME (Figure 2E) as well as KCL-induced contraction (Figure 2F). However, phenylephrine induced a significant increase in MRAs contraction in CHF-147 hamster (Figure 2G).

### *The δ-sarcoglycan deficiency induce a decrease in NO and FAK pathway*

To understand the mechanism that modifies vascular reactivity, the proteins expression of the eNOS pathway was studied in MRAs (Figure 3). Globally, the shear stress pathway indicators were not modified in the δ-sarcoglycan deficient MRAs. However, the phosphorylation of eNOS Ser1177 was significantly

decreased (Figure 3G and I). In addition, δ-sarcoglycan deficient MRAs were characterized by significant decrease in the FAK and RhoA expression (Figure 3B and 3J, respectively).

***The decrease in FMD due to δ-sarcoglycan deficiency is caused by increased oxidative stress, iNOS and COX-2***

The strong attenuation of mechanotransduction properties of the MRAs led us to study related oxidative stress and inflammatory factors. We tested the possibility that the diminished FMD could be caused by the production of reactive oxygen species (ROS) or cyclooxygenase (COX). In the whole tissue, MRA presented a significant increase in p47phox expression (Figure 4A). In addition, when treated by DHE for ROS observation, MRAs isolated from the δ-sarcoglycan deficient hamsters showed a greater signal in the endothelium compared to control (Figure 4B). Endothelial cells also presented a significant increase in COX-2 and iNOS expression (Figure 4C and D, respectively). Furthermore, the SOD mimetic Tempol (Figure 4E) significantly improved FMD in CHF-147 hamsters, while the COX-2 inhibitor NS398 (Figure 4F) showed a non-significant improvement.

# DISCUSSION

This study demonstrated selective alteration of flow (shear stress)-dependent mechanotransduction in the mesenteric resistance arteries of young CHF-147 hamsters without cardiomyopathy (δ-sarcoglycan-deficient hamster) due to increased oxidative stress.

Resistance arteries, subjected to mechanical forces, develop a highly autoregulated tone to locally adapt the blood flow supply in order to meet organ needs (15). Flow-mediated dilation plays a key role in the control of resistance artery tone, and consequently, in the control of local blood flow (16). A change in the balance between vasodilator and vasoconstrictor influences may alter the blood flow supply and induce tissue damage, such as that observed in δ-sarcoglycan-deficient hamsters (5). In this latter study, histological analysis suggested the presence of coronary vasospasm, which was suppressed by vasodilator treatment. This study provides a potential explanation for these observations. The vasoconstrictor tone in MRAs was modified with an increased alpha-adrenergic tone. Flow-mediated dilation was severely reduced without a change in the dilatory capacity of smooth muscle cells (sodium nitroprusside-induced dilation) or in the basal production of NO. Decreased FMD is the hallmark of endothelial dysfunction, and an early decrease in FMD has been described in most cardiovascular diseases (such as coronary disease (17) and hypertension (18)), metabolic syndrome (19) and diabetes (20). Thus, our findings provide a rational explanation for the vascular disorder accompanying cardiomyopathy in old animals in δ-sarcoglycan-deficient hamsters. In addition, the early decline in FMD occurring before any alteration in cardiac function, play certainly a role in the development of cardiac disorders.

We previously showed that dystrophin plays a role in FMD. Indeed, in mdx mice lacking functional dystrophin, FMD is strongly and selectively attenuated (21) and treatment with gentamicin (which allows recovery of the protein) restores FMD to a normal level (22). In addition, vascular remodeling due to a chronic increase in blood flow is attenuated in mdx mice (10). The results of the present study strengthen the assumption that the mechanotransduction of shear stress by endothelial cells involves the sarcoglycan-dystrophin complex. Nevertheless, the link between this complex and eNOS activation remains unclear. In fact, the PI3 kinase-Akt pathway selectively activates endothelial cell NO production

in response to shear stress (23, 24). Nevertheless, in the present study, this pathway was not affected by the absence of δ-sarcoglycan. The main differences between the studies are the type of cells used (cultured cells in the referenced studies versus whole blood vessels with quiescent cells in our present study) and the type of response observed with a direct measurement of dilation in our present study. Although eNOS expression was not lower in δ-sarcoglycan-deficient hamsters, its phosphorylation level was decreased. Arteries were rapidly collected from the hamsters after sacrifice and quickly frozen before analysis. Thus, our finding that eNOS phosphorylation was low in CHF-147 hamsters is in agreement with our observation that FMD was reduced. Flow (shear stress) is the main endogenous regulator of eNOS expression. We also found that oxidative stress, COX-2 and iNOS expression were increased in MRAs from δ-sarcoglycan-deficient hamsters. This is in agreement with previous studies that have shown the involvement of ROS in the pathogenesis of muscular dystrophy (25). INOS is associated with increased catabolic activity and co-expressed with pro-inflammatory cytokines and adhesion molecules during muscle injury and wasting (26). Unlike other forms of NOS, this isoform is not regulated by the calcium ion, but is primarily induced by ROS and inflammatory cytokines via the activation of NFκB and the MAPKinase pathway in skeletal muscle (27). In the endothelium and due to the decrease in FMD, high levels of NO are required to compensate for this decrease, which can lead to the formation of peroxynitrite, a highly reactive species that contributes to oxidative damage. Under these conditions of increased oxidative stress, it has been described that the generation of ROS and the formation of peroxynitrite further activate COX-2, explaining this increase in hamsters deficient for δ-sarcoglycan (28, 29).–In addition, we demonstrated an increase of p47phox in CHF-147 endothelial cells. P47phox is a subunit of the NADPH oxidase (NADPHox) complex, involved in the production of H2O2. But the mechanism by which δ-sarcoglycan mutation increases p47phox level is not clear. We can hypothesize that the δ-sarcoglycan mutation may disrupt cellular signaling pathways, leading to increased transcription of the gene encoding p47phox (transcriptional regulation) (30). Then, mutation may affect the stability of p47phox mRNA or its translation rate (post-transcriptional regulation). Finally, the δ-sarcoglycan mutation may alter protein degradation mechanisms, leading to accumulation of p47phox (post-translational regulation). Another hypothesis is that δ-sarcoglycan mutations may increase oxidative stress (31) and inflammation in endothelial cells. This could trigger a compensatory response, increasing the expression of components of the NADPHox system, including p47phox. Finally, δ-sarcoglycan mutations affect the stability of the plasma membrane (32).

This could indirectly influence the regulation of p47phox, which is involved in the function of NADPHox at the membrane (disruption of membrane stability). Further research would be needed to elucidate the precise mechanism.

In skeletal muscles, ROS contribute to membrane protein nitrosylation and muscle cell inflammation. ROS and COX-2 are also associated with alterations in the endothelium and smooth muscle-dependent tone in the vascular wall. Although ROS levels were higher in CHF-147 hamsters than in control animals, the main difference between hamster types was found in FMD. Decreasing ROS levels with SOD-mimetic tempol significantly improved FMD in CHF-147 hamsters without affecting the wild-type. However, specific inhibition of COX-2 by NS-398 did not significantly improve FMD in CHF-147 hamsters although ROS and COX-2 derivatives showed an increase in CHF-147 hamsters and as previously shown in the context of arterial dysfunction (33–36), demonstrating their involvement in reducing FMD.

In conclusion, the present study demonstrated that specific vascular disorders affect mechanotransduction in CHF-147 hamster MRAs, with a reduction in flow-mediated dilation. The involvement of ROS and inflammation in resistance arteries endothelium may be of interest for the treatment of vascular disorders and ischemic events in patients with muscular dystrophy or sarcoglycanopathy.

# GLOSSARY

Ach : Acetylcholine
COX : Cyclooxygenase
eNOS : Endothelial nitric oxide synthase
FMD : Flow-mediated dilation
iNOS : Inducible nitric oxide synthase
MRA : Mesenteric resistance arteries
PE : Phenylephrine
ROS : Reactive oxygen species
SNP : Sodium nitroprusside

# DATA AVAILABILITY

The data, methods used in the analysis, and materials used to conduct the study are available from the corresponding author upon reasonable request. Requests to access the datasets should be directed to laurent.loufrani@inserm.fr.

# ACKNOWLEDGMENTS

We thank SCAHU (an animal facility in Angers) which takes care of the animals.

Alexis Richard: UMR CNRS 6015, INSERM U1083, MitoVasc Institute, University of Angers, France.
Arnaud Bocquet: UMR CNRS 6015, INSERM U1083, MitoVasc Institute, University of Angers, France.
Eric Belin de Chantemèle: Vascular Biology Center, Medical College of Georgia at Augusta University,United States of America; Department of Medicine, Medical College of Georgia at Augusta University, United States of America.
Kevin Retailleau: UMR CNRS 6015, INSERM U1083, MitoVasc Institute, University of Angers, France.
Bertrand Toutain: UMR CNRS 6015, INSERM U1083, MitoVasc Institute, University of Angers, France.
Héloïse Mongue-Din: NMR Laboratory, Neuromuscular Investigation Center, Institute of Myology, Paris, France.
Anne-Laure Guihot: UMR CNRS 6015, INSERM U1083, MitoVasc Institute, University of Angers, France.
Celine Fassot: UMR CNRS 6015, INSERM U1083, MitoVasc Institute, University of Angers, France.
Daniel Henrion: UMR CNRS 6015, INSERM U1083, MitoVasc Institute, University of Angers, France.
Yves Fromes: NMR Laboratory, Neuromuscular Investigation Center, Institute of Myology, Paris, France.
Laurent Loufrani UMR CNRS 6015, INSERM U1083, MitoVasc Institute, University of Angers, France.

# GRANTS

This work was supported in part by a grant from the Association Française contre la Myopathie (AFM, Paris, France, grant 2012).

Arnaud Bocquet was supported a fellowships of the Conseil général du Maine et Loire (N2006-09).
Kevin Retailleau was supported by a fellowship, 2009-09 Angers Loire Metropole.

## DISCLOSURES

The funders had no role in study design, data collection and analysis, decision to publish, or preparation of the manuscript and no additional external funding received for this study.

## DISCLAIMERS

None

## AUTHOR CONTRIBUTIONS

Alexis Richard: prepared figures, drafted manuscript, approved final version of manuscript.
Arnaud Bocquet: performed experiments, analyzed data, prepared figures, approved final version of manuscript.
Eric Belin de Chantemèle: performed experiments, analyzed data, prepared figures, approved final version of manuscript.
Kevin Retailleau: performed experiments, analyzed data, prepared figures, approved final version of manuscript.
Bertrand Toutain: performed experiments, analyzed data, approved final version of manuscript.
Héloïse Mongue-Din: performed experiments, analyzed data, approved final version of manuscript.
Anne-Laure Guihot: performed experiments, analyzed data, approved final version of manuscript.
Celine Fassot: edited and revised manuscript, approved final version of manuscript, approved final version of manuscript.
Daniel Henrion: edited and revised manuscript, approved final version of manuscript.
Yves Fromes: edited and revised manuscript, approved final version of manuscript.
Laurent Loufrani: Conceived and designed research, interpreted results of experiments, prepared figures, drafted manuscript, edited and revised manuscript, approved final version of manuscript.

## REFERENCES

1. **Lim LE**, **Campbell KP**. The sarcoglycan complex in limb-girdle muscular dystrophy. *Curr Opin Neurol* 11: 443–452, 1998. doi: 10.1097/00019052-199810000-00006.

2. **Bushby KM**. The limb-girdle muscular dystrophies-multiple genes, multiple mechanisms. *Hum Mol Genet* 8: 1875–1882, 1999. doi: 10.1093/hmg/8.10.1875.

3. **Wheeler MT**, **Allikian MJ**, **Heydemann A**, **Hadhazy M**, **Zarnegar S**, **McNally EM**. Smooth muscle cell-extrinsic vascular spasm arises from cardiomyocyte degeneration in sarcoglycan-deficient cardiomyopathy. *J Clin Invest* 113: 668–675, 2004. doi: 10.1172/JCI20410.

4. **Coral-Vazquez R**, **Cohn RD**, **Moore SA**, **Hill JA**, **Weiss RM**, **Davisson RL**, **Straub V**, **Barresi R**, **Bansal D**, **Hrstka RF**, **Williamson R**, **Campbell KP**. Disruption of the sarcoglycan-sarcospan complex in vascular smooth muscle: a novel mechanism for cardiomyopathy and muscular dystrophy. *Cell* 98: 465–474, 1999. doi: 10.1016/s0092-8674(00)81975-3.

5. **Cohn RD**, **Durbeej M**, **Moore SA**, **Coral-Vazquez R**, **Prouty S**, **Campbell KP**. Prevention of cardiomyopathy in mouse models lacking the smooth muscle sarcoglycan-sarcospan complex. *J Clin Invest* 107: R1-7, 2001. doi: 10.1172/JCI11642.

6. **Lipskaia L**, **Pinet C**, **Fromes Y**, **Hatem S**, **Cantaloube I**, **Coulombe A**, **Lompré A-M**. Mutation of delta-sarcoglycan is associated with Ca(2+) -dependent vascular remodeling in the Syrian hamster. *Am J Pathol* 171: 162–171, 2007. doi: 10.2353/ajpath.2007.070054.

7. **Mulvany MJ**, **Aalkjaer C**. Structure and function of small arteries. *Physiol Rev* 70: 921–961, 1990. doi: 10.1152/physrev.1990.70.4.921.

8. **Fromes Y**, **Gaillard D**, **Ponzio O**, **Chauffert M**, **Gerhardt M-F**, **Deleuze P**, **Bical OM**. Reduction of the inflammatory response following coronary bypass grafting with total minimal extracorporeal circulation. *Eur J Cardio-Thorac Surg Off J Eur Assoc Cardio-Thorac Surg* 22: 527–533, 2002. doi: 10.1016/s1010-7940(02)00372-x.

9. **Hunter EG**, **Hughes V**, **White J**. Cardiomyopathic hamsters, CHF 146 and CHF 147: a preliminary study. *Can J Physiol Pharmacol* 62: 1423–1428, 1984. doi: 10.1139/y84-236.

10. **Loufrani L**, **Li Z**, **Lévy BI**, **Paulin D**, **Henrion D**. Excessive microvascular adaptation to changes in blood flow in mice lacking gene encoding for desmin. *Arterioscler Thromb Vasc Biol* 22: 1579–1584, 2002. doi: 10.1161/01.atv.0000032652.24932.1a.

11. **Halpern W**, **Mulvany MJ**. Tension responses to small length changes of vascular smooth muscle cells [proceedings]. *J Physiol* 265: 21P-23P, 1977.

12. **Belin de Chantemèle EJ**, **Retailleau K**, **Pinaud F**, **Vessières E**, **Bocquet A**, **Guihot AL**, **Lemaire B**, **Domenga V**, **Baufreton C**, **Loufrani L**, **Joutel A**, **Henrion D**. Notch3 is a major regulator of vascular tone in cerebral and tail resistance arteries. *Arterioscler Thromb Vasc Biol* 28: 2216–2224, 2008. doi: 10.1161/ATVBAHA.108.171751.

13. **Bagi Z**, **Toth E**, **Koller A**, **Kaley G**. Microvascular dysfunction after transient high glucose is caused by superoxide-dependent reduction in the bioavailability of NO and BH(4). *Am J Physiol Heart Circ Physiol* 287: H626-633, 2004. doi: 10.1152/ajpheart.00074.2004.

14. **Bouvet C**, **Belin de Chantemèle E**, **Guihot A-L**, **Vessières E**, **Bocquet A**, **Dumont O**, **Jardel A**, **Loufrani L**, **Moreau P**, **Henrion D**. Flow-induced remodeling in resistance arteries from obese Zucker rats is associated with endothelial dysfunction. *Hypertens Dallas Tex 1979* 50: 248–254, 2007. doi: 10.1161/HYPERTENSIONAHA.107.088716.

15. **Bevan JA**, **Henrion D**. Pharmacological implications of the flow-dependence of vascular smooth muscle tone. *Annu Rev Pharmacol Toxicol* 34: 173–190, 1994. doi: 10.1146/annurev.pa.34.040194.001133.

16. **Loufrani L**, **Henrion D**. Role of the cytoskeleton in flow (shear stress)-induced dilation and remodeling in resistance arteries. *Med Biol Eng Comput* 46: 451–460, 2008. doi: 10.1007/s11517-008-0306-2.

17. **Varin R**, **Mulder P**, **Tamion F**, **Richard V**, **Henry JP**, **Lallemand F**, **Lerebours G**, **Thuillez C**. Improvement of endothelial function by chronic angiotensin-converting enzyme inhibition in heart failure : role of nitric oxide, prostanoids, oxidant stress, and bradykinin. *Circulation* 102: 351–356, 2000. doi: 10.1161/01.cir.102.3.351.

18. **Pinaud F**, **Bocquet A**, **Dumont O**, **Retailleau K**, **Baufreton C**, **Andriantsitohaina R**, **Loufrani L**, **Henrion D**. Paradoxical role of angiotensin II type 2 receptors in resistance arteries of old rats. *Hypertens Dallas Tex 1979* 50: 96–102, 2007. doi: 10.1161/HYPERTENSIONAHA.106.085035.

19. **Suzuki T**, **Hirata K**, **Elkind MSV**, **Jin Z**, **Rundek T**, **Miyake Y**, **Boden-Albala B**, **Di Tullio MR**, **Sacco R**, **Homma S**. Metabolic syndrome, endothelial dysfunction, and risk of cardiovascular events: the Northern Manhattan Study (NOMAS). *Am Heart J* 156: 405–410, 2008. doi: 10.1016/j.ahj.2008.02.022.

20. **Irace C**, **Tschakovsky ME**, **Carallo C**, **Cortese C**, **Gnasso A**. Endothelial dysfunction or dysfunctions? Identification of three different FMD responses in males with type 2 diabetes. *Atherosclerosis* 200: 439–445, 2008. doi: 10.1016/j.atherosclerosis.2007.12.036.

21. **Loufrani L**, **Matrougui K**, **Gorny D**, **Duriez M**, **Blanc I**, **Lévy BI**, **Henrion D**. Flow (shear stress)-induced endothelium-dependent dilation is altered in mice lacking the gene encoding for dystrophin. *Circulation* 103: 864–870, 2001. doi: 10.1161/01.cir.103.6.864.

22. **Loufrani L**, **Dubroca C**, **You D**, **Li Z**, **Levy B**, **Paulin D**, **Henrion D**. Absence of dystrophin in mice reduces NO-dependent vascular function and vascular density: total recovery after a treatment with the aminoglycoside gentamicin. *Arterioscler Thromb Vasc Biol* 24: 671–676, 2004. doi: 10.1161/01.ATV.0000118683.99628.42.

23. **Dimmeler S**, **Assmus B**, **Hermann C**, **Haendeler J**, **Zeiher AM**. Fluid shear stress stimulates phosphorylation of Akt in human endothelial cells: involvement in suppression of apoptosis. *Circ Res* 83: 334–341, 1998. doi: 10.1161/01.res.83.3.334.

24. **Fulton D**, **Gratton JP**, **McCabe TJ**, **Fontana J**, **Fujio Y**, **Walsh K**, **Franke TF**, **Papapetropoulos A**, **Sessa WC**. Regulation of endothelium-derived nitric oxide production by the protein kinase Akt. *Nature* 399: 597–601, 1999. doi: 10.1038/21218.

25. **Whitehead NP**, **Yeung EW**, **Allen DG**. Muscle damage in mdx (dystrophic) mice: role of calcium and reactive oxygen species. *Clin Exp Pharmacol Physiol* 33: 657–662, 2006. doi: 10.1111/j.1440-1681.2006.04394.x.

26. **Schulze PC**, **Gielen S**, **Schuler G**, **Hambrecht R**. Chronic heart failure and skeletal muscle catabolism: effects of exercise training. *Int J Cardiol* 85: 141–149, 2002. doi: 10.1016/s0167-5273(02)00243-7.

27. **Adams V**, **Nehrhoff B**, **Späte U**, **Linke A**, **Schulze PC**, **Baur A**, **Gielen S**, **Hambrecht R**, **Schuler G**. Induction of iNOS expression in skeletal muscle by IL-1beta and NFkappaB activation: an in vitro and in vivo study. *Cardiovasc Res* 54: 95–104, 2002. doi: 10.1016/s0008-6363(02)00228-6.

28. **Camacho M**, **López-Belmonte J**, **Vila L**. Rate of vasoconstrictor prostanoids released by endothelial cells depends on cyclooxygenase-2 expression and prostaglandin I synthase activity. *Circ Res* 83: 353–365, 1998. doi: 10.1161/01.res.83.4.353.

29. **Zou MH**, **Ullrich V**. Peroxynitrite formed by simultaneous generation of nitric oxide and superoxide selectively inhibits bovine aortic prostacyclin synthase. *FEBS Lett* 382: 101–104, 1996. doi: 10.1016/0014-5793(96)00160-3.

30. **Campbell MD**, **Witcher M**, **Gopal A**, **Michele DE**. Dilated cardiomyopathy mutations in δ-sarcoglycan exert a dominant-negative effect on cardiac myocyte mechanical stability. *Am J Physiol Heart Circ Physiol* 310: H1140-1150, 2016. doi: 10.1152/ajpheart.00521.2015.

31. **Ramirez-Sanchez I**, **De los Santos S**, **Gonzalez-Basurto S**, **Canto P**, **Mendoza-Lorenzo P**, **Palma-Flores C**, **Ceballos-Reyes G**, **Villarreal F**, **Zentella-Dehesa A**, **Coral-Vazquez R**. (-)-Epicatechin improves mitochondrial-related protein levels and ameliorates oxidative stress in dystrophic δ-sarcoglycan null mouse striated muscle. *FEBS J* 281: 5567–5580, 2014. doi: 10.1111/febs.13098.

32. **Chen J**, **Jin Y**, **Wang H**, **Wei S**, **Chen D**, **Ying L**, **Zhou Q**, **Li G**, **Li J**, **Gao J**, **Kato N**, **Hu W**, **Li Y**, **Wang Y**. A haplotype of two novel polymorphisms in δ-Sarcoglycan gene increases risk of dilated cardiomyopathy in mongoloid population. *PloS One* 10: e0145602, 2015. doi: 10.1371/journal.pone.0145602.

33. **Widlansky ME**, **Price DT**, **Gokce N**, **Eberhardt RT**, **Duffy SJ**, **Holbrook M**, **Maxwell C**, **Palmisano J**, **Keaney JF**, **Morrow JD**, **Vita JA**. Short- and long-Term COX-2 inhibition reverses endothelial dysfunction in patients with hypertension. *Hypertension* 42: 310–315, 2003. doi: 10.1161/01.HYP.0000084603.93510.28.

34. **Vessières E**, **Guihot A-L**, **Toutain B**, **Maquigneau M**, **Fassot C**, **Loufrani L**, **Henrion D**. COX-2-derived prostanoids and oxidative stress additionally reduce endothelium-mediated relaxation in old type 2 diabetic rats. *PLOS ONE* 8: e68217, 2013. doi: 10.1371/journal.pone.0068217.

35. **Vessieres E**, **Belin De Chantemèle EJ**, **Toutain B**, **Guihot A-L**, **Jardel A**, **Loufrani L**, **Henrion D**. Cyclooxygenase-2 inhibition restored endothelium-mediated relaxation in old obese zucker rat mesenteric arteries. *Front Physiol* 1, 2010. doi: 10.3389/fphys.2010.00145.

36. **Félétou M**, **Huang Y**, **Vanhoutte PM**. Endothelium-mediated control of vascular tone: COX-1 and COX-2 products. *Br J Pharmacol* 164: 894–912, 2011. doi: 10.1111/j.1476-5381.2011.01276.x.

# FIGURE LEGENDS

**Figure 1. Flow-induced dilation is attenuated in mesenteric arteries from CHF-147 hamsters.** Changes in diameter in response to flow changes when pressure was maintained at 75 mmHg and after 50% of basal diameter contraction with PE, in mesenteric resistance arteries from control and CHF-147 hamsters (N=11 WT, N=8 CHF-147). Values are mean ± SEM. 2-way RM-ANOVA was used.

**Figure 2. Mesenteric arteries from CH-147 hamsters did not show any changes in their vascular structure and reactivity.** (A) Pressure-diameter (passive arterial diameter) relationship determined in mesenteric resistance arteries (N=11 WT, N=8 CHF-147); (B) Media cross sectional area in mesenteric resistance arteries, which were measured under a pressure of 75 mmHg. Arteries were isolated from control and

CHF-147 hamsters (N=9 WT, N=4 CHF-147). (C) Endothelium dependent and (D) independent dilation after phenylephrine preconstriction ($10^{-6}$M) (N=9 WT, N=4 CHF-147); (E) Concentration-dependent inhibition of NO synthesis by L-NAME after phenylephrine preconstriction ($10^{-6}$M) (N=9 WT, N=4 CHF-147); (F) KCL (N=9 WT, N=4 CHF-147) and (G) phenylephrine induced contraction ($10^{-9}$-$10^{-4}$ M) (N=9 WT, N=4 CHF-147). Values are mean ± SEM. 2-way RM-ANOVA was used for curves, and Mann Whitney test for histograms.

**Figure 3**. **NO and FAK pathway are decreased in mesenteric arteries from CH-147 hamsters. (A)** Immunoblots of focal adhesion kinase (FAK), PI3K, AKT, eNOS, RhoA, and the phosphorylated form (p) of eNOS and Akt in mesenteric resistance arteries from control and CHF-147 hamsters. (B) FAK (N=5 WT, N=3 CHF-147), (C) PI3K (N=3 WT, N=3 CHF-147), (D) p-AKT (N=4 WT, N=3 CHF-147), (E) AKT (N=7 WT, N=6 CHF-147), (F) p-AKT/AKT ratio (N=7 WT, N=3 CHF-147), (G) p-eNOS (N=6 WT, N=3 CHF-147), (H) eNOS (N=6 WT, N=3 CHF-147), (I) p-eNOS/eNOS ratio (N=6 WT, N=3 CHF-147), (J) RhoA (N=4 WT, N=4 CHF-147) relative expression to β-actin (same loading control as presented in Figure 4). Values are mean ± SEM. Mann Whitney test was used.

**Figure 4. Increased endothelial superoxide production associated with COX-2 and iNOS expression induce an alteration in flow-mediated dilation in mesenteric arteries from CHF-147 hamsters.** (A) p47phox protein quantification in whole mesenteric artery (N=5 WT, N=4 CHF-147), relative expression to β-actin (same loading control as presented in Figure 3). (B) Reactive oxygen species (ROS) visualized using DHE staining (N=4 WT, N=4 CHF-147), (C) COX-2 (N=4 WT, N=4 CHF-147) and (D) iNOS immunofluorescence staining in endothelium of mesenteric arteries from control and CHF-147 hamsters (N=5 WT, N=5 CHF-147). (E) Flow-induced dilation in mesenteric arteries in hamsters treated chronically with tempol or water (N=5 WT, N=5 CHF-147, N=5 WT+Tempol, N=5 CHF-147+Tempol). (F) Flow-induced dilation in isolated mesenteric arteries treated with NS-398 (COX-2 inhibitor) (N=3 WT, N=4 CHF-147, N=4 WT+NS-398, N=4 CHF-147+NS-398). Values are mean ± SEM. Mann Whitney test was used for A-D panels, 2-way RM-ANOVA was used for E and F panels.

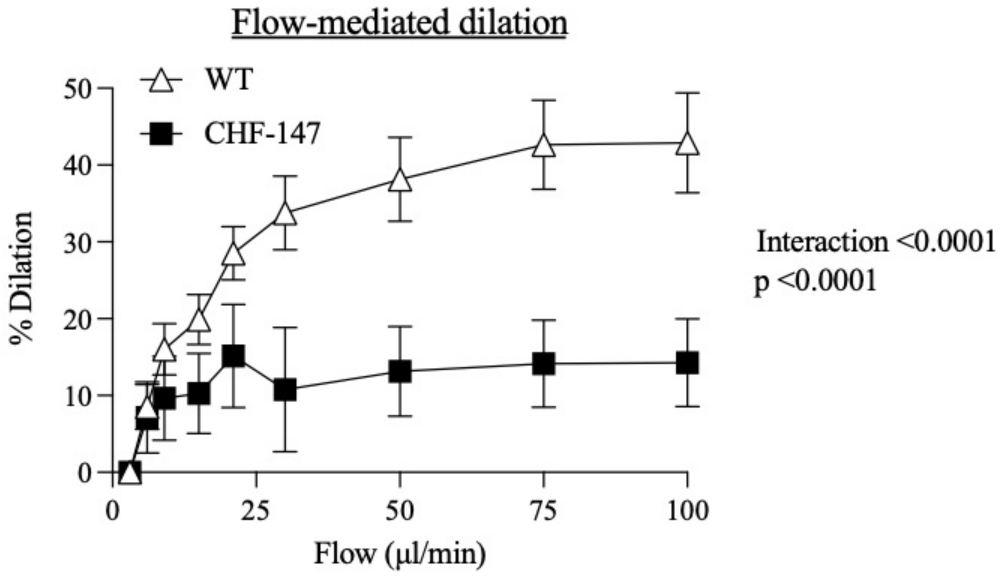
Flow-mediated dilation
WT
CHF-147
% Dilation
50
40
30
20
10
0
0
25
50
75
100
Flow (µl/min)
Interaction <0.0001
p <0.0001

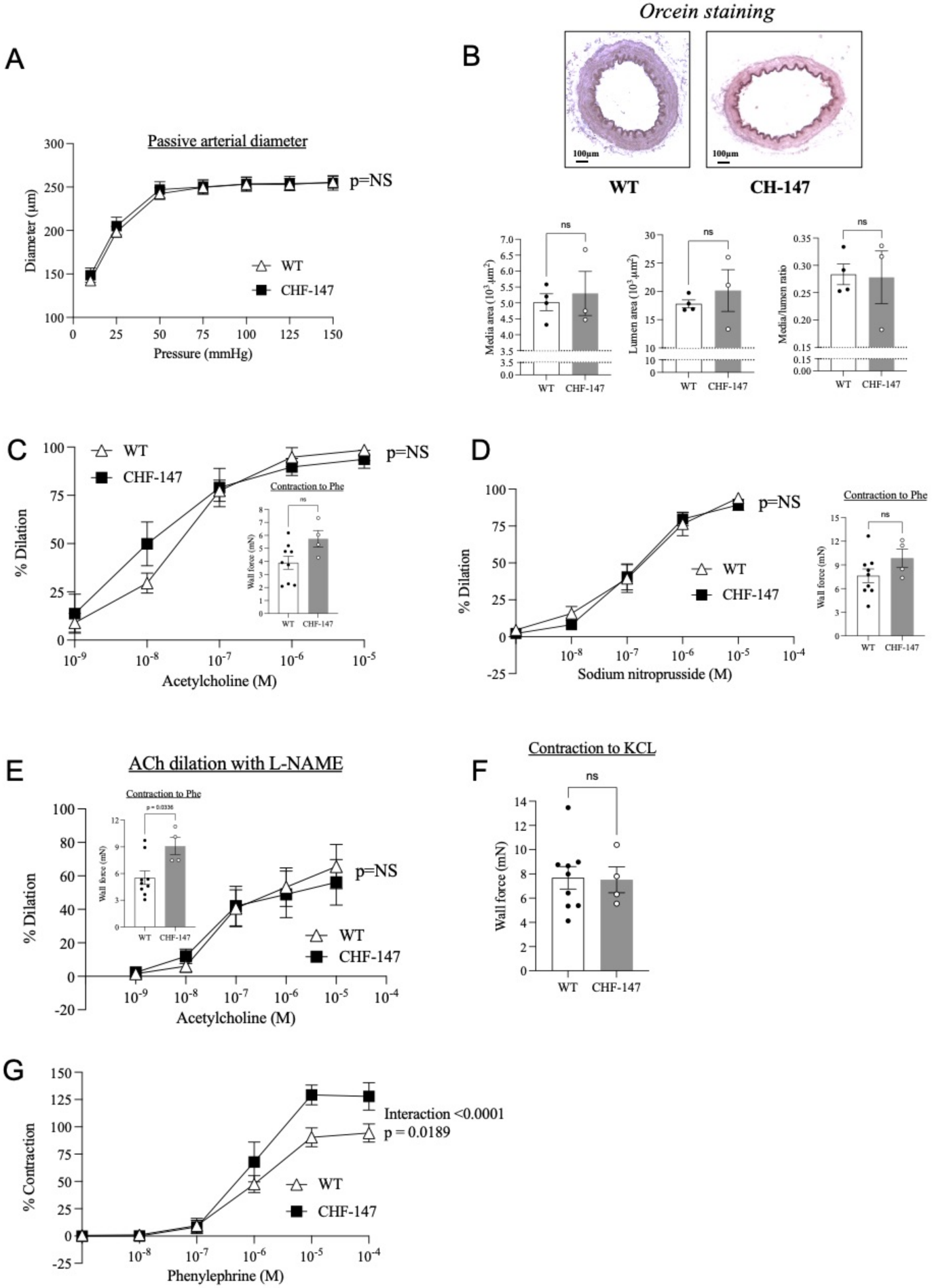
A
Passive arterial diameter
Diameter (µm)
Pressure (mmHg)
WT
CHF-147
p=NS
B
Orcein staining
100µm
WT
CH-147
Media area (10³ µm²)
Lumen area (10³ µm²)
Media/lumen ratio
ns
C
% Dilation
Acetylcholine (M)
p=NS
Contraction to Phe
Wall force (mN)
D
% Dilation
Sodium nitroprusside (M)
p=NS
Contraction to Phe
E
ACh dilation with L-NAME
% Dilation
Acetylcholine (M)
p=NS
Contraction to Phe
F
Contraction to KCL
Wall force (mN)
G
% Contraction
Phenylephrine (M)
Interaction <0.0001
p = 0.0189

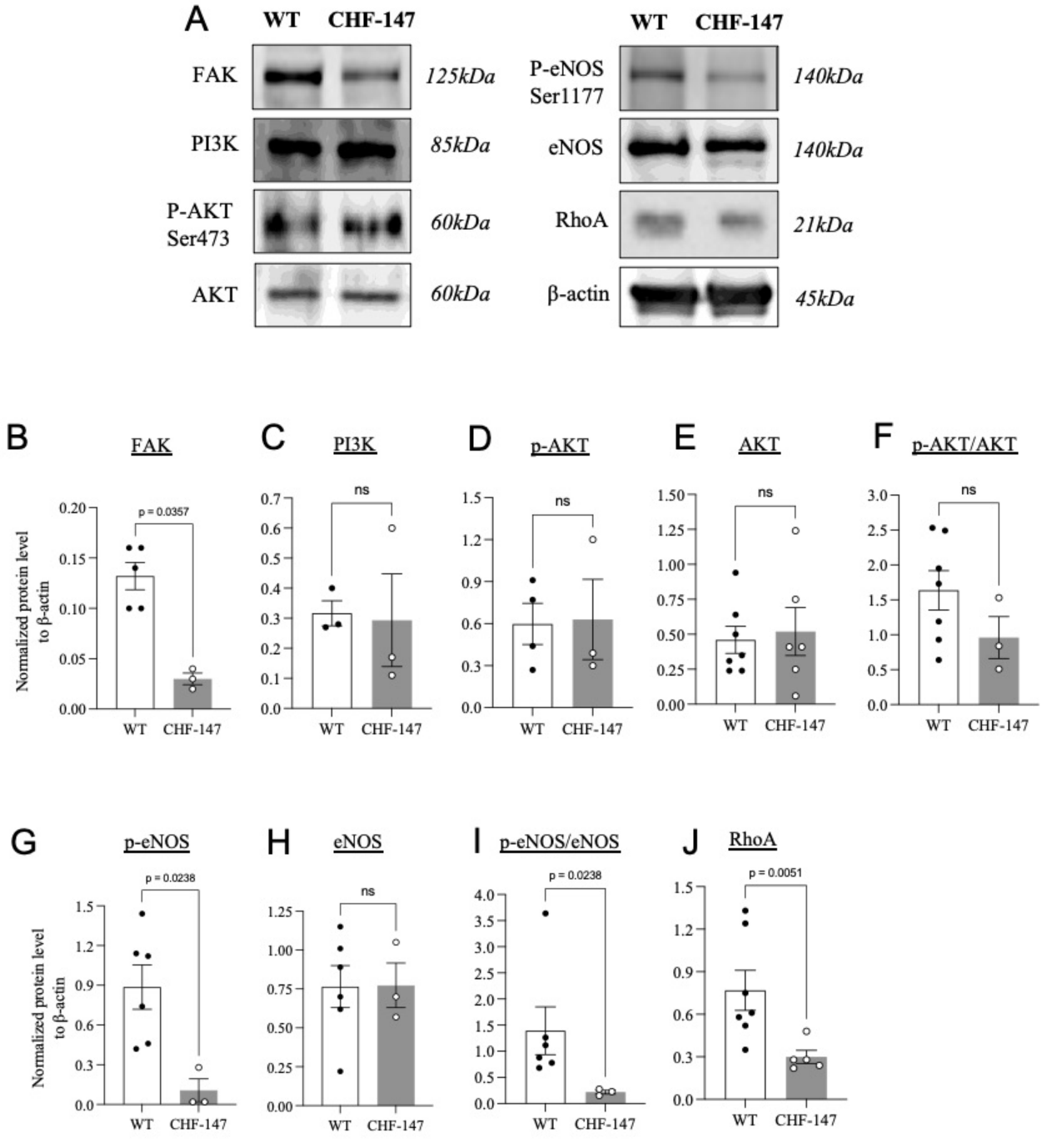
A
WT
CHF-147
FAK
125kDa
PI3K
85kDa
P-AKT Ser473
60kDa
AKT
60kDa
P-eNOS Ser1177
140kDa
eNOS
140kDa
RhoA
21kDa
β-actin
45kDa
B
FAK
C
PI3K
D
p-AKT
E
AKT
F
p-AKT/AKT
Normalized protein level to β-actin
p = 0.0357
ns
G
p-eNOS
H
eNOS
I
p-eNOS/eNOS
J
RhoA
p = 0.0238
p = 0.0051

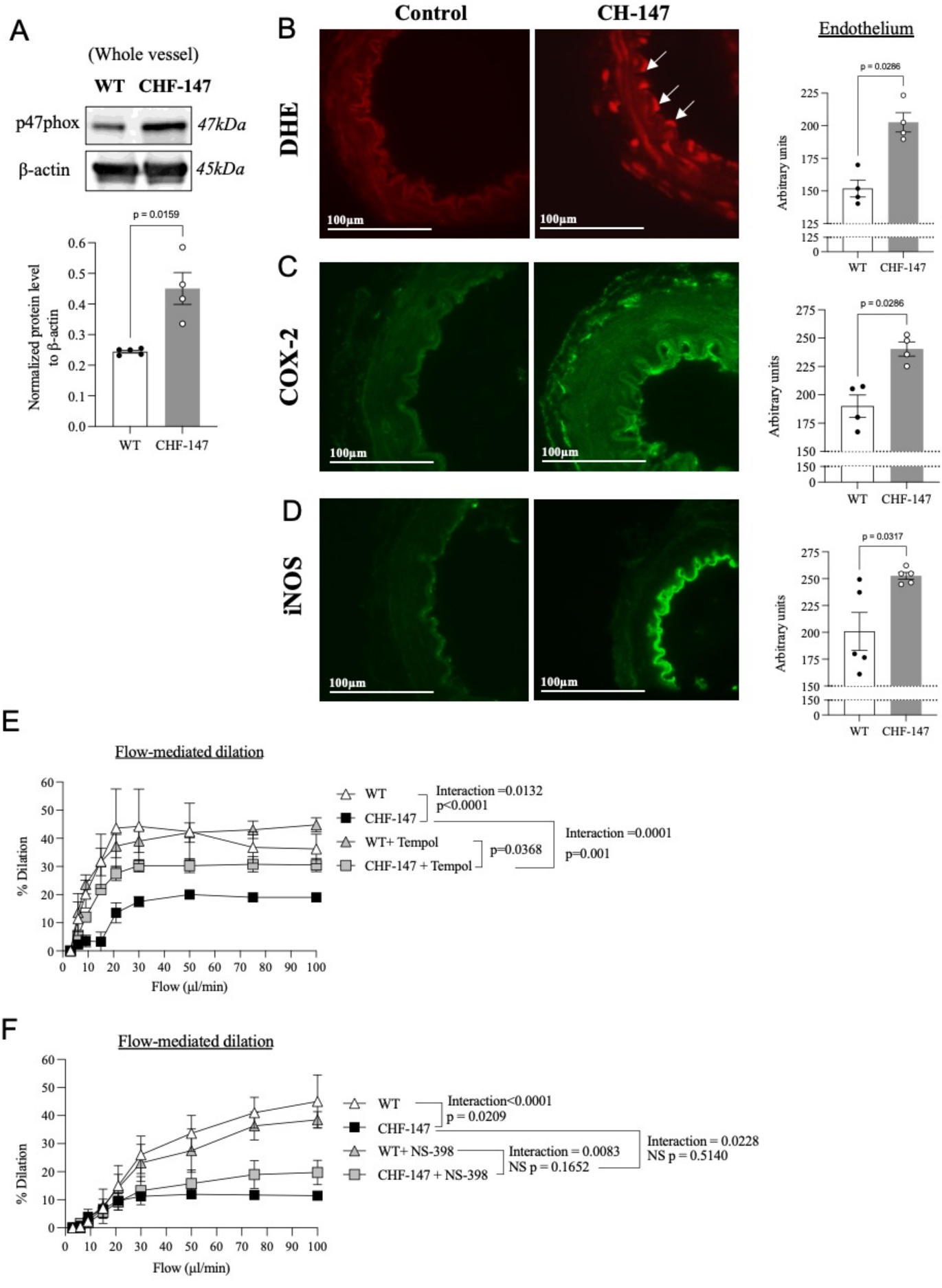
A
(Whole vessel)
WT CHF-147
p47phox
47kDa
β-actin
45kDa
p = 0.0159
Normalized protein level to β-actin
WT CHF-147
B
Control
CH-147
DHE
100µm
Endothelium
p = 0.0286
Arbitrary units
WT CHF-147
C
COX-2
p = 0.0286
D
iNOS
p = 0.0317
E
Flow-mediated dilation
% Dilation
Flow (µl/min)
WT
CHF-147
WT+ Tempol
CHF-147 + Tempol
Interaction =0.0132
p<0.0001
p=0.0368
Interaction =0.0001
p=0.001
F
Flow-mediated dilation
WT+ NS-398
CHF-147 + NS-398
Interaction<0.0001
p = 0.0209
Interaction = 0.0083
NS p = 0.1652
Interaction = 0.0228
NS p = 0.5140